**Open Access**
**Baghdad Science Journal** **Vol.16 (Special Issue) 2019**

DOI: http://dx.doi.org/10.21123/bsj.2019.16.2(SI).0504

# A Comparative Analysis of the Zernike Moments for Single Object Retrieval

*Suraya Abu Bakar*[*] *Muhammad Suzuri Hitam*[**]
*Wan Nural Jawahir Hj Wan Yussof****

Received 17/9/2018, Accepted 12/11/2018, Published 20/6/2019



**Abstract:**

Zernike Moments has been popularly used in many shape-based image retrieval studies due to its powerful shape representation. However its strength and weaknesses have not been clearly highlighted in the previous studies. Thus, its powerful shape representation could not be fully utilized. In this paper, a method to fully capture the shape representation properties of Zernike Moments is implemented and tested on a single object for binary and grey level images. The proposed method works by determining the boundary of the shape object and then resizing the object shape to the boundary of the image. Three case studies were made. Case 1 is the Zernike Moments implementation on the original shape object image. In Case 2, the centroid of the shape object image in Case 1 is relocated to the center of the image. In Case 3, the proposed method first detect the outer boundary of the shape object and then resizing the object to the boundary of the image. Experimental investigations were made by using two benchmark shape image datasets showed that the proposed method in Case 3 had demonstrated to provide the most superior image retrieval performances as compared to both the Case 1 and Case 2. As a conlusion, to fully capture the powerful shape representation properties of the Zernike moment, a shape object should be resized to the boundary of the image.

**Key words**: shape features, shape image retrieval, Zernike Moments

## Introduction:

With the increasing importance of images in people’s daily life, the latest technologies of image retrieval based on shape has been widely studied. Shape features give significant information of the images such as the position and size. Hence, image retrieval based on shape is crucial in various applications such as medical imaging, automation systems and the remote sensing. For example, in medical imaging, shape retrieval is used for the retrieval of the MRI human spine images (1), brains (2,3) and pulmonary nodules lung (4). The use of relevant shape features are important to the radiologists for their record in evaluating and diagnosis of the medical image database.

Many researchers have utilized shape features in various applications including content-based image retrieval (5,6,7,8) and trademark (9,10,11,12,13).

Universiti Malaysia Terengganu, Malaysia
Corresponding author:[*]surayag@gmail.com
[**]suzuri@umt.edu.my
[***]wannurwy@umt.edu.my

Among the three main image features characteristics, shape is a fundamental feature which provides significant information of the image in terms of size, position and shape of an objects. The shape of objects play a pivotal role among the different aspects of visual information. Therefore, a shape feature is a very powerful feature when used in image similarity search and retrieval. Unlike color and texture features, the shape of an object is linked closely to the object identity or functionality. Therefore, shape-based image retrieval is an important topic and the authors attempted to develop an alternative method to existing shape image descriptors in this paper.

In (14), proposed an algorithm called histogram-based contrast and spatial information-enhanced region-based contrast that can effectively extract important object features. They claimed that their algorithm achieved superior retrieval rate as compared to other methods. Nowadays, 3D shape image retrieval has received much attention in many computer vision applicatons such as in shape recognition, object detection and graphics areas. Several methods exist and used for 3D shape retrieval such as Convolutional Neural Networks (15,16), deep learning feature (17), bag-of-features (18) and Cross-Domain Manifold Ranking (19). The goal of Convolutional Neural Networks (CNNs) is to represent the hierarchy of feature representation (16) and the learning of CNN is based on Stochastic Gradient Descent (SGD) (20). (21) used CNN to learn a general similarity function for image patches and their approach shows that it can significantly outperform the other shape-based methods on several problems.

Some image retrieval approaches used bag-of-features approach by computing the global and local descriptors of the shape before they are used for object similarity retrieval. (18) shows that by combining both features with multiview shape matching scheme, it can significantly outperforms other methods for 3D shape matching. (19) proposed an algorithm for the retrieval of sketch based 3D model that compare features from 3D model and features from hand-rawn sketches. However, 2D images are still popularly been used today in most of the applications for extracting the shape features because of the complex and high computational nature in 3D shapes. Hence, this paper focuses on how to further enhance the properties of Zernike Moments that will provide a solution for the fundamental problem of shapes feature representation and only focuses on 2D images.

**Zernike Moments:**

Zernike Moments (22) are the most well-known orthogonal moments that are able to store the image information with minimal information redundancy. Zernike Moments are claimed to be rotation invariant and robust to noise (23). Generally, a Zernike Moment that is defined over the polar coordinated inside a unit circle of order *p* can be mathematically written as in Eq. (1).

$$Z_{pq} = \frac{(\int \; p+1)}{\pi} \int_0^{2\pi}\int_0^{1} V_{pq} * (r,\theta) f(r,\theta) r \quad dr \quad d\theta, \quad r \leq 1 \quad \dots(1)$$

The function $V_{pq}(r,\theta)$ represents Zernike polynomials of order *p* with repetition *q* and $*$ represents complex conjugate. Let consider *N* as the number of pixels at both image axes. Equation (1) can be rewritten in a discrete form as follows:

$$Z_{pq} = \frac{(p+1)}{\pi (N-1)^2} \sum_{x=1}^{N}\sum_{y=1}^{N} V_{pq} * (r,\theta) \;\; f(x,y) \quad ..(2)$$

where $r = (x^2 + y^2)^{1/2} / N$ and $\theta = \tan^{-1}(y/x)$. Zernike polynomials $V_{pq}(r,\theta)$ of order *p* are defined as functions of the polar coordinates $r,\theta$ as in Eq.(3).

$$V_{pq}(r,\theta) = R_{pq}(r) e^{iq\theta} \qquad (3)$$

where $R_{pq}(r)$ is real-valued radial polynomial given by Eq.(4).

$$R_{pq}(r) = \sum_{s=0}^{(p-|q|)/2} (-1)^s \frac{(p-s)!}{s!\left(\frac{p-2s+|q|}{2}\right)! \left(\frac{p-2s-|q|}{2}\right)!} \; r^{p-2s}$$

…(4)

where $p = 0,1,2,\ldots,\infty;\ 0 \leq |q| \leq p;$ and $p-|q|$ is even. Due to the nature of Zernike Moments that is defined in polar coordinates and image is defined in a Cartesian space, we need to perform a square to circular transformation for the image as illustrated in Figure 1 (24) before Zernike Moments can be computed. After the transformation, the Cartesian coordinate system in image *I(x, y)* can be represented by new image in polar coordinate, I( $\gamma,\xi$ ) where $\gamma$ denoted the radius of the circle and $\xi$ the position index of the pixel on the circle.

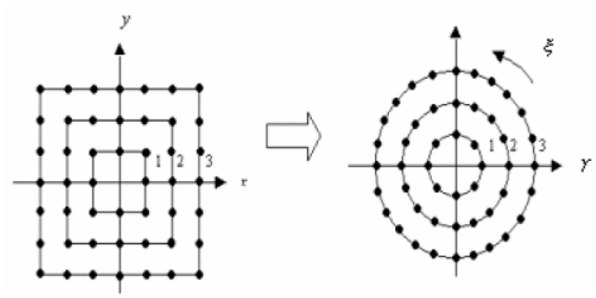


**Figure 1. Cartesian Image Space to Polar Coordinates Transformation(24).**

**System Framework of Zernike Moments**

Figure 2 ilustrates the system framework of Zernike Moments implementation that is used in this paper. There are two main phases in the system implementation; offline and online phase. In the offline phase, the Zernike Moments properties were initially extracted from shape image dataset and later stored stored as feature vector. In the online phase, a user can select any query image from the shape image database. The algorithm will compute the Zernike Moments features from the query image. These set of features were later be compared with the set of previously stored features. By using Euclidean distance similarity measurement, the distance between the features from the query image and each of the respective feature vector in the feature database were computed. The distance measurement will later be sorted and the image with the smallest distance value represents the closet image to the query image.

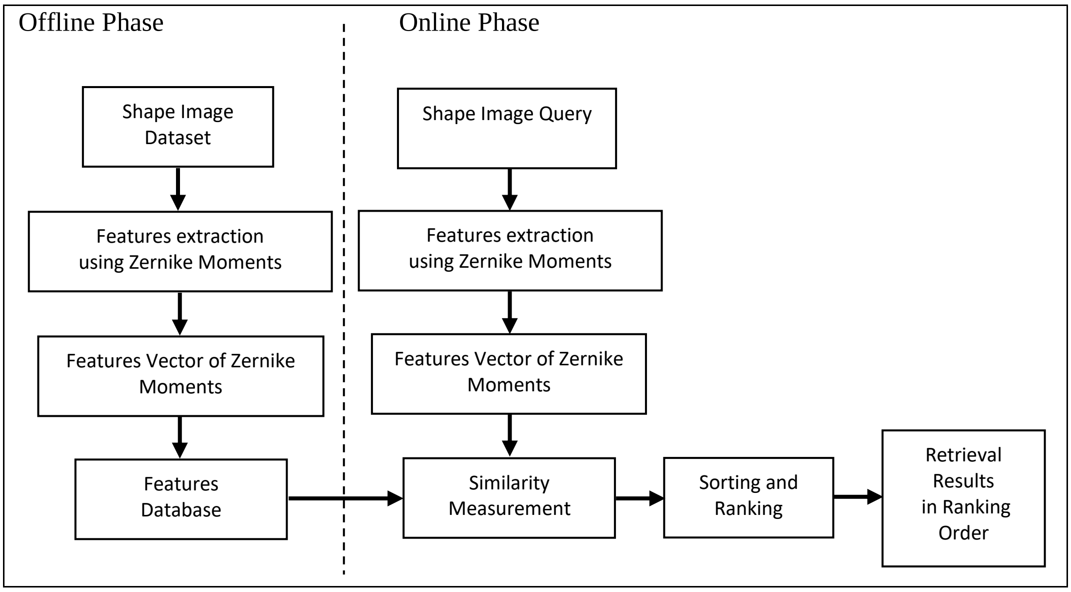


**Figure 2. System Framework of the Zernike Moments Method for Image Retrieval.**

### Feature Extraction using Zernike Moments

The experimental investigations have been carried out to analyse the capability of Zernike Moments to represent a single object shape and its robustness to image transformation for image retrieval. The aim of these experiments is to explore the shape retrieval capabilities of Zernike Moments for three case studies. In this paper, Zernike Moments ($Z_{pq}$) of order 10 is used throughout the experiment as shown in Table 1.

**Table 1. Illustration of Zernike Moments for *p*=10 and *q*=10.**

| ***q*** / ***p*** | **0** | **1** | **2** | **3** | **4** | **5** | **6** | **7** | **8** | **9** | **10** |
|---|---|---|---|---|---|---|---|---|---|---|---|
| **0** | $Z_{00}$ | - | | | | | | | | | |
| **1** | - | $Z_{11}$ | | | | | | | | | |
| **2** | $Z_{20}$ | - | $Z_{22}$ | | | | | | | | |
| **3** | - | $Z_{31}$ | - | $Z_{33}$ | | | | | | | |
| **4** | $Z_{40}$ | - | $Z_{42}$ | - | $Z_{44}$ | | | | | | |
| **5** | - | $Z_{51}$ | - | $Z_{53}$ | - | $Z_{55}$ | | | | | |
| **6** | $Z_{60}$ | - | $Z_{62}$ | - | $Z_{64}$ | - | $Z_{66}$ | | | | |
| **7** | - | $Z_{71}$ | - | $Z_{73}$ | - | $Z_{75}$ | - | $Z_{77}$ | | | |
| **8** | $Z_{80}$ | - | $Z_{82}$ | - | $Z_{84}$ | - | $Z_{86}$ | - | $Z_{88}$ | | |
| **9** | - | $Z_{91}$ | - | $Z_{93}$ | - | $Z_{95}$ | - | $Z_{97}$ | - | $Z_{99}$ | |
| **10** | $Z_{100}$ | - | $Z_{102}$ | - | $Z_{104}$ | - | $Z_{106}$ | - | $Z_{108}$ | - | $Z_{1010}$ |

## The Proposed Method:

Figure 3 illustrates the workflow process for the three case studies of Zernike Moments implementation namely Case 1, Case 2 and Case 3. In Case 1, Zernike Moments properties were directly extracted from the shape image. Whereas, for Case 2 and Case 3, before the computation of Zernike Moments, an additional image preprocessing is made to the input image. In Case 2, the algorithm first compute the centroid of the object shape and based on this centroid value, the object is moved to the center of the image. In Case 3, the skeletonizing algorithm is first applied to the input image. Based on these computed skeleton of the object, the minimum and the maximum horizontal and vertical boundaries of the object is determined. By using these boundaries, the object shape is cropped and later resize into standard image dimension that is used in this paper, i.e. 256 x 256.

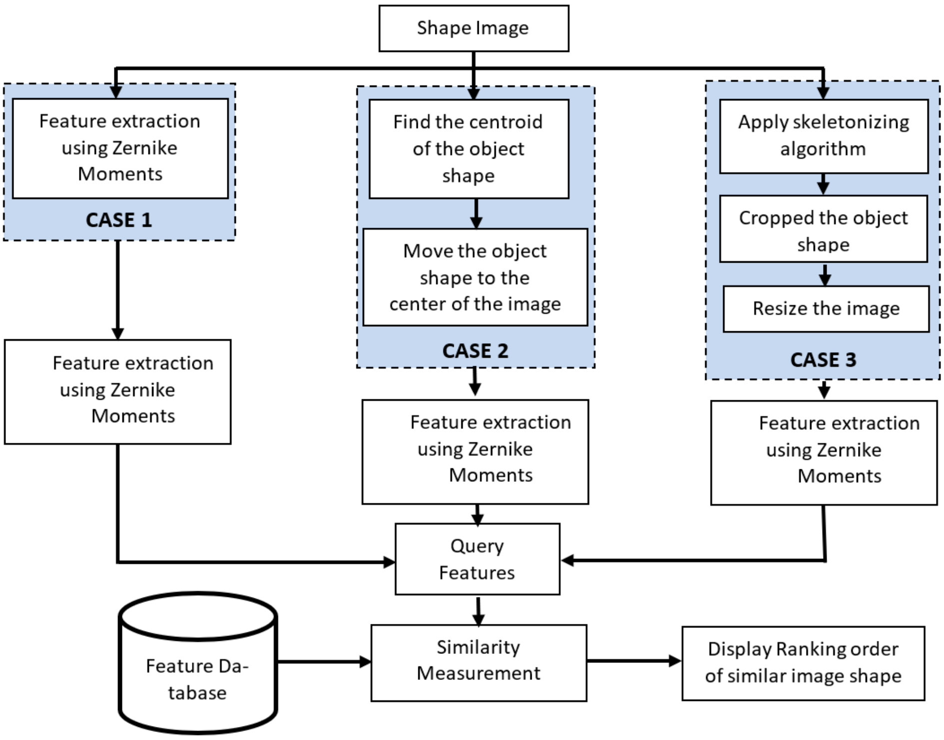


**Figure 3. The Proposed Three Case Studies of Zernike Moments Implementation.**

## Zernike Moments Implementation of Case 1

In Case 1, the Zernike Moments method is applied to test the shape based image retrieval capability using the whole image. The workflow process for Case 1 implementation is shown in Figure 4.

First, the process starts with an input image from the shape image database, showing an apple image from MPEG-7 Core Experiment Shape-1 Part B. The second step is the calculation of global Zernike Moments on the input image. The image is computed and a total of 36 features Zernike Moments from order 0 to 10 were extracted on the image. Then, the features are measured and compared with the features in the database. Finally, the results will be displayed accordingly in ranking orders.

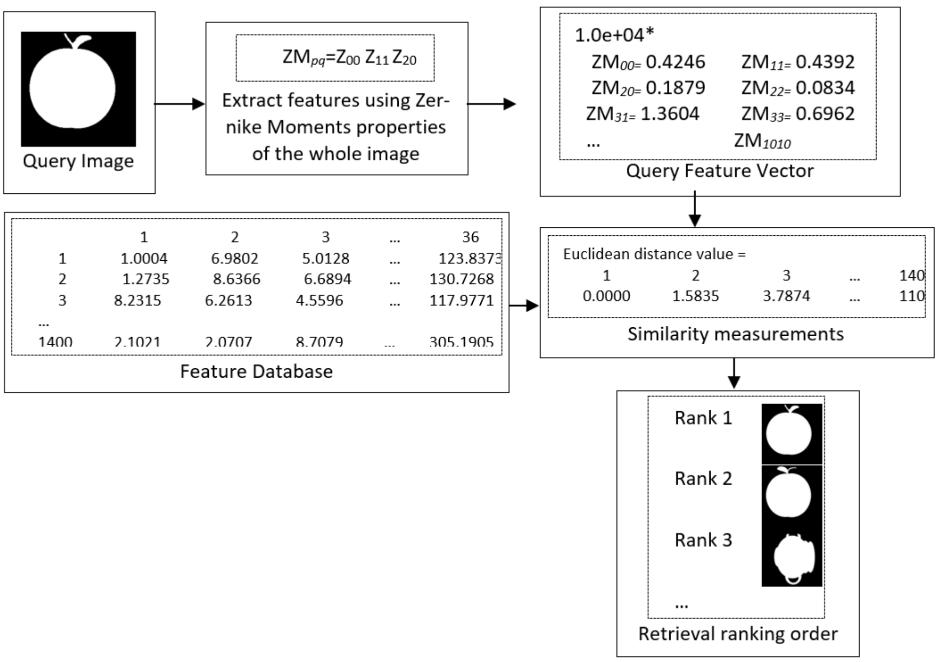


**Figure 4. Case 1 Implementation Process.**

**Zernike Moments Implementation of Case 2**

In this case, the Zernike Moments method is implemented by computing the centroid of the object shape and by using this value, the object is relocated to the center of the image. Figure 5 shows the workflow process of the Case 2. For the workflow process in Fig. 5, it can be seen that there are an additional two processes as compared with workflow process for Case 1. The first one is the process to compute the centroid of the object shape from the input image. In the illustration, the detected centroid, *c* for brick image is shown in the second process of the figure. This process is one of the many important steps due to detect a shape of an object without distortion. Then, by using the centroid points of the object shape, the object is relocated to the center of the image.

This proposed process can be considered as one of the steps to normalize the image before the computation of the image features. After that, the same process as in Case 1 were applied until the retrieval ranking results are displayed accordingly. However, Case 2 extracts an unused area of the object image. Waste information fills up the unused area that affects the image features. This leads to the proposed Case 3.

**Zernike Moments Implementation of Case 3**

To fully capture the object shape features, Case 3 is proposed. In Case 3 implementation, it covers surrounding area of the object shape to get the features information. For the purpose of the Zernike Moments implementation investigations, Case 3 implementation used three steps of image preprocessing,i.e. skeletonizing process, shape cropping process and image resizing process. The workflow process as shown in Figure 6 gives details of these three processes and shows the overall steps process of Case 3 implementation.

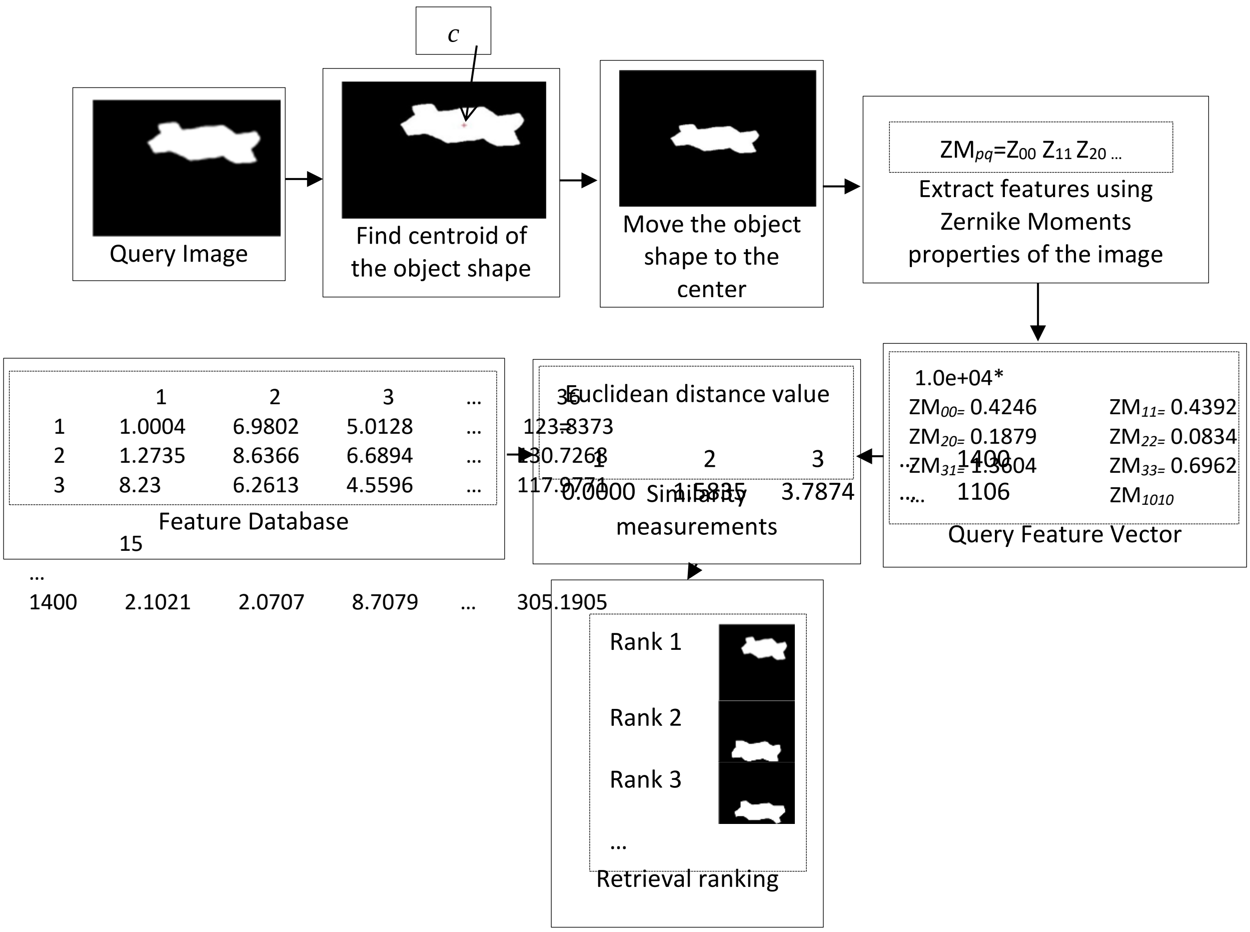


**Figure 5. Case 2 Implementation Process.**

Figure 6 illustrates a hammer image as the input image or also known as query image in demonstrating the process in Case 3 implementation. To compute the skeleton of the shape object image and its endpoints, the skeletonizing algorithm is applied over the input image. The result of the hammer image after the morphological process is shown in the second workflow diagram. The start points and endpoints later on will be useful in determining the maximum and minimum values for the shape object image to be cropped. After this process, the third step in this figure shows the hammer shape that is already been cropped. Then, the image is resized into 256 by 256 dimensions to make it uniform with other images in Case 1 and Case 2.

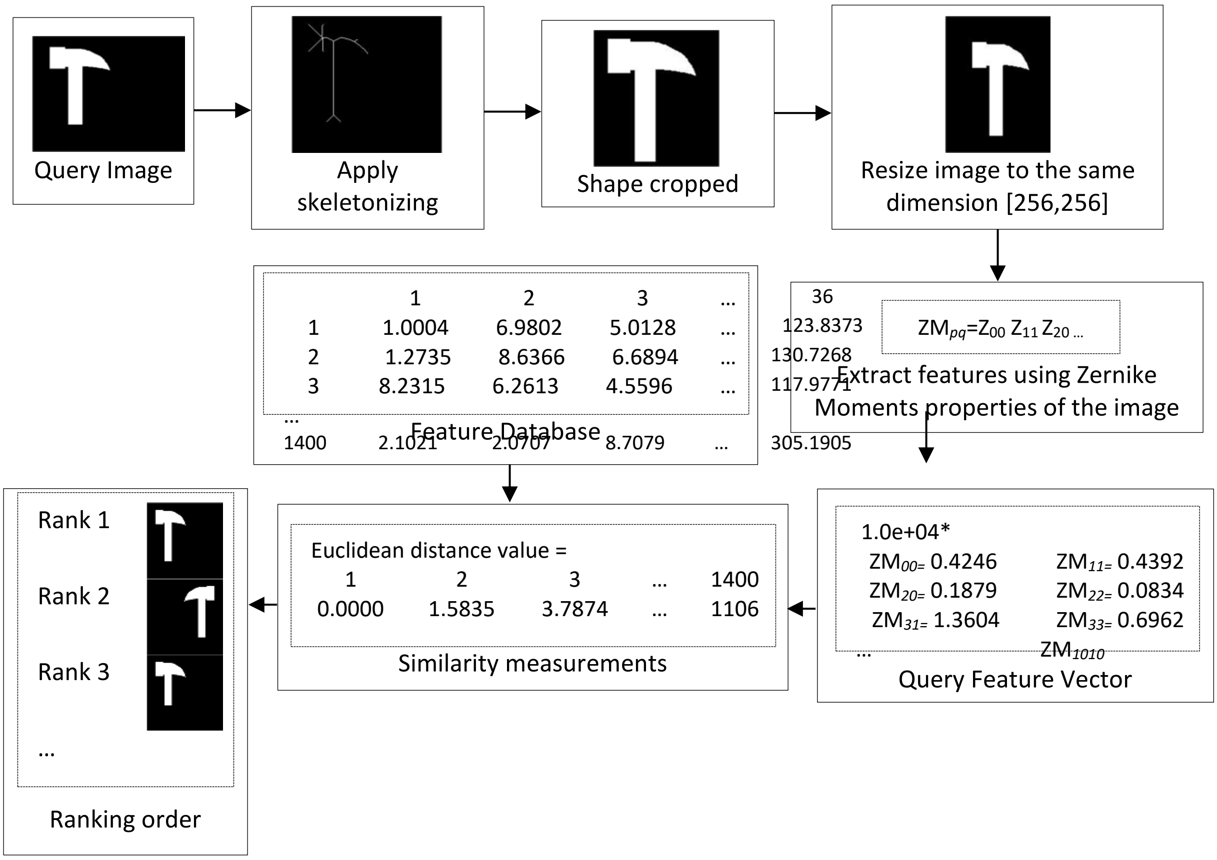


**Figure 6. Case 3 Implementation Process.**

**Retrieval Results**

During the retrieval process, Zernike Moments features of each query image are compared with those of the images in the image features database. The features were matches with the respective features in order to rank each indexed image according to its distance to the query image and display its results. In this section, retrieval ranking results of Zernike Moments using the MPEG-7 Core Experiment Shape-1 Part B and Columbia Object Image Library (COIL-20) dataset are presented.

MPEG-7 Core Experiment Shape-1 Part B dataset contains 1400 binary images. Table 2 shows the top ten retrieval ranking results of an apple-1 shape object. From this table, it can be observed that the query had correctly retrieved the similar category object in the first and second rank of all the case studies. For Case 1 implementation, the similar apple image category are able to be retrieved in the first top two ranking only. It failed to retrieve similar image category under rank 3 until rank 10. From the retrieval results in Case 2 implementation, it can be observed that it successfully retrieved similar image category in the first third rank but failed to retrieved correct image categories at rank 4 and rank 5. In rank 6 until rank 8, it retrieves the similar image category again. However, in rank 9, it again retrieved a different category. Then at rank tenth, it retrieved similar image category again. Case 3 retrieval results show that it perfectly retrieved the similar image category in the first 9th rank and only failed to retrieve similar image category under rank 10.

**Table 2. Top Ten Retrieval Ranking Results of an Apple-1 Image.**

| Ranking / Method | Rank 1 | Rank 2 | Rank 3 | Rank 4 | Rank 5 | Rank 6 | Rank 7 | Rank 8 | Rank 9 | Rank 10 |
|---|---|---|---|---|---|---|---|---|---|---|
| **Case 1** |  |  |  |  |  |  |  |  |  |  |
| **Case 2** |  |  |  |  |  |  |  |  |  |  |
| **Case 3** |  |  |  |  |  |  |  | 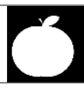 |  |  |

Overall from the comparison retrieval results, the retrieval ranking results in Case 3 provide the best retrieval ranking as compared with the Case 1 and the Case 2. Only the top ten image retrieval results were displayed in Table 2 due to space limitation. To give the overall retrieval ranking results, Figure 7(a) shows the precision and recall graph for Case 1, Case 2 and Case 3 as illustrated using red, green and blue marker, respectively. The cubic spline interpolation is employed throughout this paper for smoother curve. The graph shown in Figure 7(a) indicates that Case 3 gives the best retrieval results as compared with Case 1 and Case 2 from the beginning of the retrieval ranking results.

This retrieval results also shows that the retrieval produced by Case 1 is the poorest of all cases.

The precision and recall graph shown in Figure 7(b) shows the comparison of retrieval performance of Beetle-1 image from MPEG-7 dataset with the three case studies. As shown in red lines graph, Case 1 performance also provides poorest retrieval results as compared with the other two cases. In Case 2, the graph shows a better retrieval performances as compared to Case 1 but it slightly decreased along with the decreasing number of retrieved images. As can be observed, the Case 3 implementation provides the best retrieval results as compared with other two casess. However, it is slightly decreased at the end of the retrieval.

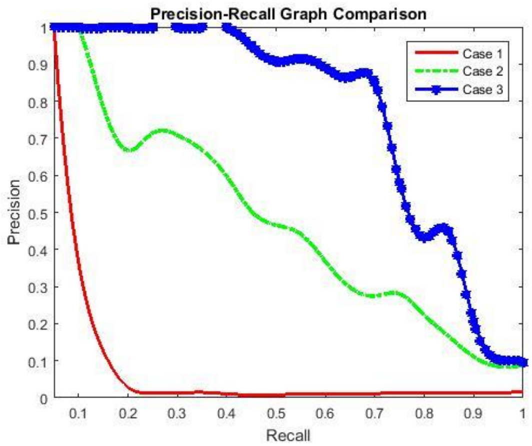


**(a) Apple image**

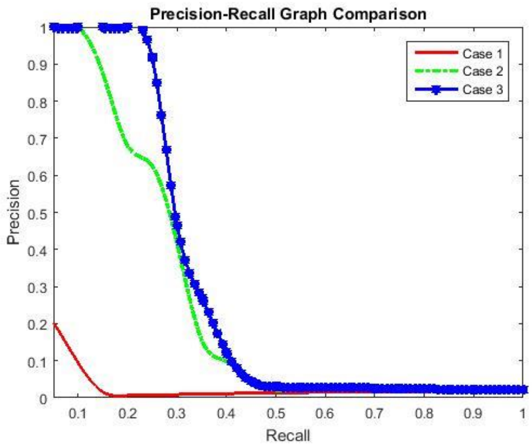


**(b) Beetle image**

**Figure 7. Precision-Recall Graph for MPEG-7 dataset image.**

In addition, the top ten retrieval ranking results for another sample images on MPEG-7 dataset for Case 3 is presented as in Table 3. It contains the retrieval ranking results for six categories of images including car, bone, cup, device, face and heart. As can be observed, Case 3 implementation perfectly retrieved similar categories for the first top ten ranks under the category of car, bone, face and heart. For cup and device category, it successfully retrieved similar image category from rank 1 to rank 8 and it only failed to retrieve similar category images under rank 9.

**Table 3. Retrieval Ranking Results of Case 3 Implementation on MPEG-7 Dataset.**

| IMAGE QUERY | RETRIEVAL RANKING RESULTS | | | | | | | | | |
|---|---|---|---|---|---|---|---|---|---|---|
| | Rank 1 | Rank 2 | Rank 3 | Rank 4 | Rank 5 | Rank 6 | Rank 7 | Rank 8 | Rank 9 | Rank 10 |

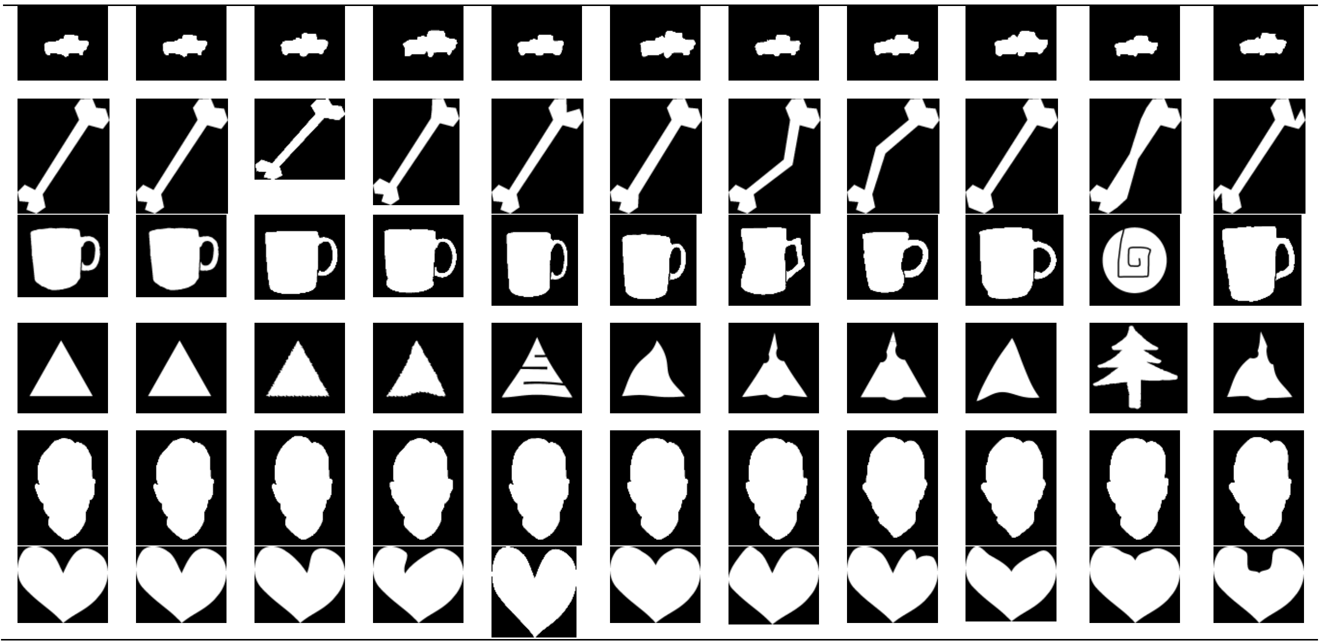

Columbia Object Image Library (COIL-20) dataset is a collection of gray scale images which contains 1440 images for 20 different objects. Some sample of retrieval ranking results for Case 3 implementation including object 5, 6, 7, 8, 17 and object 20 image category in COIL-20 dataset are displayed in Table 4. From the top ten retrieval ranking results, it can be concluded that Case 3 implementation results gives good retrieval under all categories, where it can be supported by the results shown in Table 4 that it perfectly retrieved similar category for all top ten ranks.

From the top ten retrieval ranking results in Table 4, it shows that Case 3 gives the superior retrieval ranking where it perfectly retrieved similar category of object in COIL-20 dataset. The results obtained from the COIL-20 dataset retrieval ranking are better as compared to MPEG-7 dataset. One of the reasons is COIL-20 dataset includes 70 similar images under one category and MPEG-7 dataset only have 20 similar images for each category. Thus, the chances for COIL-20 dataset to retrieve similar category are bigger than MPEG-7 dataset retrieval ranking results.

The precision and recall graph of COIL-20 image example is shown in Figure 8. The graph in Figure 8(a) indicates that Case 3 implementation represented by blue markers gives superior performance as compared with Case 1 and Case 2. From the graph in Figure 8(b), it can be seen that the retrieval performance decreases for Case 1 along with the decreasing number of retrieved similar images. In Case 2, the retrieval performance decreased in the middle of the performance as shown in green lines graph. Case 3 gives best retrieval performance as compared with the other two cases where it perfectly retrieved the similar image category from the beginning of the retrieval and it performances only decreases toward the end of the retrieval.

**Table 4. Retrieval Ranking Results of Case 3 Implementation on MPEG-7 Dataset.**

| IMAGE QUERY | RETRIEVAL RANKING RESULTS | | | | | | | | | |
|---|---|---|---|---|---|---|---|---|---|---|
| | Rank 1 | Rank 2 | Rank 3 | Rank 4 | Rank 5 | Rank 6 | Rank 7 | Rank 8 | Rank 9 | Rank 10 |

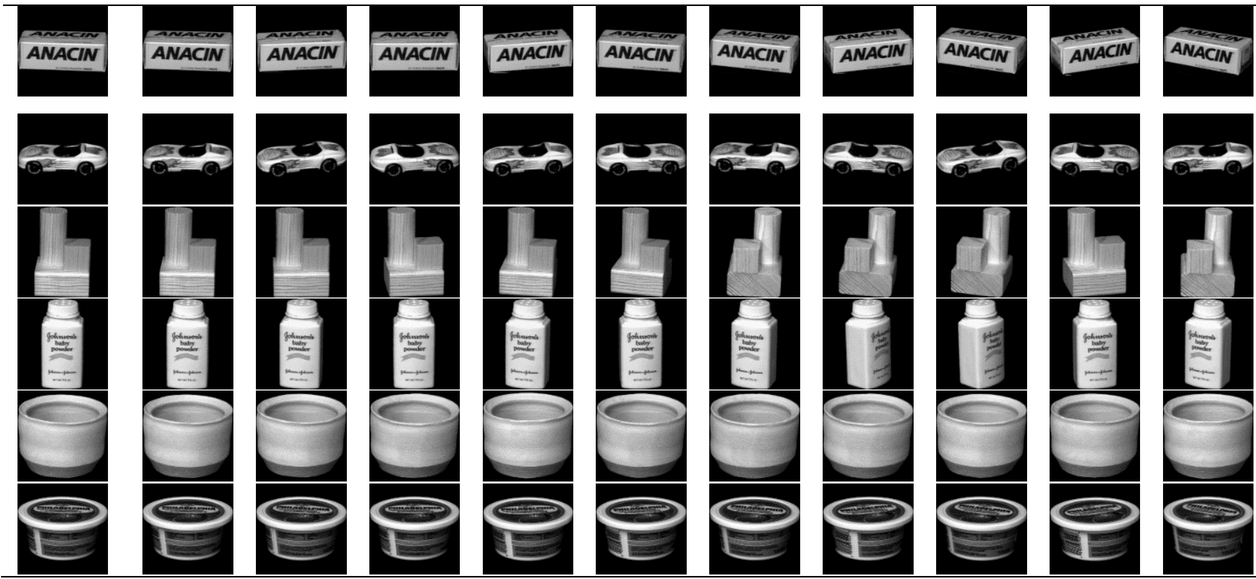


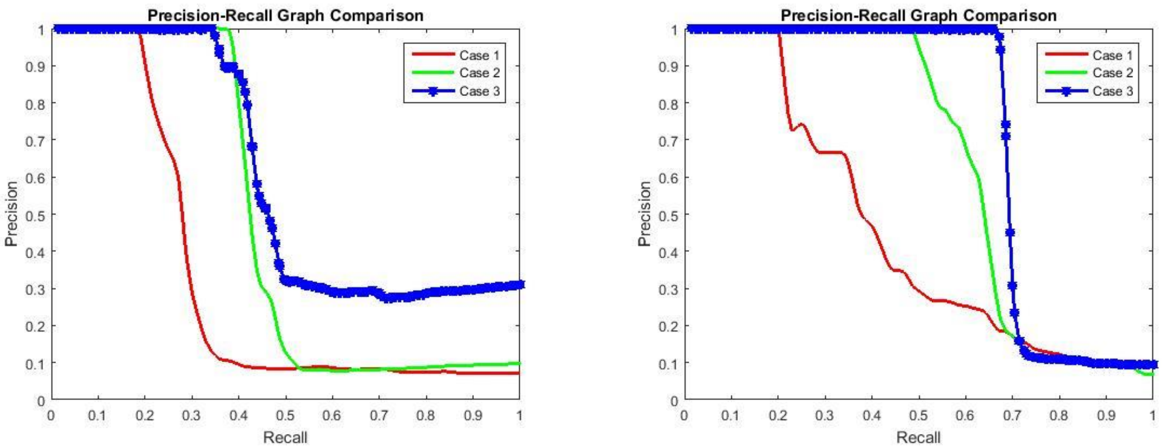


**(a) Object 2 image** **(b) Object 11 image**

**Figure 8. Precision-Recall Graph for COIL-20 Image Dataset.**

From the results, it can be concluded that to fully capture Zernike Moments properties for shape represenation, the object has to fully cover the image boundary. By moving the centroid of the object to the center of the image, it will improve the object shape representation as can be observed from Case 1 to Case 2. However, Zernike Moments properties could not fully cover the shape of the object. This lack of shape representation by Zernike Moments is clearly evidence from the retrieval results of Case 2 as compared to the retrieval results of Case 3. Even though Case 2 retrieval results are better than Case 1, some of the object shapes does not cover the image. Therefore, the shape properties of Case 2 from Zernike Moments could not fully represent the shape as compared to Case 3. By maximizing the size of the shape object as in Case 3, it proved that Zernike Moments properties could perform the best to represent the object shape. Therefore, to be practical in applying Zernike Moments method, we have to limit the coverage of the object shape to the boundary of the object. By maximizing the size of the shape object to certain area of interest, we can fully use Zernike Moments properties. For example, to locate a small size object in a panoramic image, if we want to use Zernike Moments to detect the image shape, we have to use the correct window size that fit to the object size. For a varying scale object size, then a dynamic window size has to be employed. Further investigation into these properties is subject to future research project.

## Conclusion:

This paper has presented 3 case studies of the implementation of Zernike Moments for shape based image retrieval. Case 1 is the basic conventional implementation of Zernike Moments based method and Case 2 is basically relocation of an object shape into the center of the image based on the centroid of the object. In Case 3, the actual object boundary were identified and later resized to fit the enveloped of the actual image size. From the analysis of the results, it can be concluded that the properties of Zernike Moments could be fully utilized if the image of the shape covers the enveloped of the object completely. This finding exhibited in Case 3 where the shape of the object is resized to fully cover the shape of the object. The retrieval perfomances of Case 3 performs the best out of the other 2 case studies. Therefore, to fully capture the properties of Zernike Moments, a shape object boundary should be determined and based on these boundary information, the shape object should be resized to fit the enveloped of the image. In this way, the properties of Zernike Moments can be fully captured to represent a shape object as compared to a shape object that are not fully covered in an image. It is interesting if we could utilize these information and integrate them with other features from other methods so that the more efficient shape based image retrieval could be achieved in the future.

## Notation:

| | |
|---|---|
| $p$ | positive integer or zero; i.e.: $p = 0,1,2,...,\infty$ |
| $q$ | positive integer subject to constraint; $p-\|q\|$ is even and $q \le p$ |
| $\theta$ | angle between the vector $\rho$ and the axis $x$ in the counter clockwise direction |

## Conflicts of Interest: None.

## References:


1. Ling CS, Zaki WM, Hussain A, Ahmad WS, Hing EY. Shape based image retrieval system for MRI spine. In 2017 6th International Conference on Electrical Engineering and Informatics (ICEEI), 2017 Nov 25 (pp. 1-6). IEEE.
2. Faria AV, Oishi K, Yoshida S, Hillis A, Miller MI, Mori S. Content-based image retrieval for brain MRI: An image-searching engine and population-based analysis to utilize past clinical data for future diagnosis. NeuroImage: Clinical. 2015 Jan 1;7:367-76.
3. Pandian AA, Balasubramanian R. Fusion of Contourlet Transform and Zernike Moments using Content based Image Retrieval for MRI Brain Tumor Images. Indian Journal of Science and Technology. 2016 Aug 10;9(29).
4. Dhara AK, Mukhopadhyay S, Dutta A, Garg M, Khandelwal N. Content-based image retrieval system for pulmonary nodules: Assisting radiologists in self-learning and diagnosis of lung cancer. Journal of digital imaging. 2017 Feb 1;30(1):63-77.
5. Brandt S, Laaksonen J, Oja E. Statistical shape features for content-based image retrieval. Journal of Mathematical Imaging and Vision. 2002 Sep 1;17(2):187-98.
6. Mehtre BM, Kankanhalli MS, Lee WF. Shape measures for content based image retrieval: a comparison. Information processing & management. 1997 May 1;33(3):319-37.
7. Murugan MV, Mathews MS. 2D and 3D active shape model with SURF algorithm for OBJECT retrieval: Content Based Image Retrieval. In 2013 International Conference on Advanced Computing and Communication Systems (ICACCS), 2013 Dec 19 (pp. 1-7). IEEE.
8. Wu Y, Wu Y. Shape-based image retrieval using combining global and local shape features. In International Congress on Image and Signal Processing, 2009. CISP'09. 2nd 2009 Oct 17 (pp. 1-5). IEEE.
9. Anuar FM, Setchi R, Lai YK. Trademark image retrieval using an integrated shape descriptor. Expert Systems with Applications. 2013 Jan 1;40(1):105-21.
10. Eakins JP, Boardman JM, Shields K. Retrieval of trade mark images by shape feature-the ARTISAN project, 1996.
11. Jain AK, Vailaya A. Shape-based retrieval: A case study with trademark image databases. Pattern recognition. 1998 Sep 1;31(9):1369-90.
12. Jian M, Xu L. Trademark image retrieval using wavelet-based shape features. In International Symposium on Intelligent Information Technology Application Workshops, 2008. IITAW'08. 2008 Dec 21 (pp. 496-500). IEEE.
13. Yin PY, Yeh CC. Content-based retrieval from trademark databases. Pattern Recognition Letters. 2002 Jan 1;23(1-3):113-26.
14. Cheng MM, Mitra NJ, Huang X, Torr PH, Hu SM. Global contrast based salient region detection. IEEE Transactions on Pattern Analysis and Machine Intelligence. 2015 Mar 1;37(3):569-82.
15. Su H, Maji S, Kalogerakis E, Learned-Miller E. Multi-view convolutional neural networks for 3d shape recognition. In Proceedings of the IEEE international conference on computer vision 2015 (pp. 945-953).
16. Wang F, Kang L, Li Y. Sketch-based 3d shape retrieval using convolutional neural networks. InProceedings of the IEEE Conference on Computer Vision and Pattern Recognition; 2015 (pp. 1875-1883)..
17. Zhu Z, Wang X, Bai S, Yao C, Bai X. Deep learning representation using autoencoder for 3D shape retrieval. Neurocomputing. 2016 Sep 5;204:41-50.
18. Lian Z, Godil A, Sun X. Visual similarity based 3D shape retrieval using bag-of-features. In International Conference Shape Modeling (SMI), 2010 Jun 21 (pp. 25-36). IEEE.
19. Furuya T, Ohbuchi R. Ranking on cross-domain manifold for sketch-based 3D model retrieval. In

2013 International Conference on Cyberworlds (CW), 2013 Oct 21 (pp. 274-281). IEEE.
20. LeCun Y, Bengio Y. Convolutional networks for images, speech, and time series. The handbook of brain theory and neural networks. 1995 Apr;3361(10):1995.
21. Zagoruyko S, Komodakis N. Learning to compare image patches via convolutional neural networks. In Proceedings of the IEEE Conference on Computer Vision and Pattern Recognition 2015 (pp. 4353-4361).
22. Teague MR. Image analysis via the general theory of moments. JOSA. 1980 Aug 1;70(8):920-30.
23. Liao SX, Pawlak M. On the accuracy of Zernike moments for image analysis. IEEE transactions on pattern analysis and machine intelligence. 1998 Dec;20(12):1358-64.
24. Mukundan R, Ramakrishnan KR. Moment functions in image analysis-theory and applications. World Scientific; 1998 Sep 2.

# تحليل مقارن للحظات زينرك لاسترجاع كائن منفرد

**ثريا أبو بكر** **محمد سوزوري هيتام** **وان نورال جواهر هاج وان يوسف**

جامعة ماليزيا تيرينجانو ، ماليزيا

**الخلاصة:**

تم استخدام لحظات زينرك بشكل شائع في العديد من دراسات استرجاع الصور المبنية على الأشكال بسبب تمثيلها القوي للأشكال. ومع ذلك لم يتم تسليط الضوء بوضوح على نقاط قوتها وضعفها في الدراسات السابقة. وبالتالي، لا يمكن استغلال تمثيلها القوي بشكل كامل. في هذه االدراسة، يتم تنفيذ طريقة لالتقاط خصائص تمثيل الأشكال في لحظات زينرك بالكامل وتطبيقها على كائن واحد للحصول على صور ثنائية ومستوى رمادي. تعمل الطريقة المقترحة عن طريق تحديد حدود كائن الشكل ثم تغيير حجم شكل الكائن إلى حدود الصورة. تم إجراء ثلاث دراسات حالة. الحالة 1 هي تطبيق لحظات زينرك على صورة كائن الشكل الأصلي. في الحالة 2 ، يتم نقل النقطة الوسطى لصورة كائن الشكل في الحالة 1 إلى مركز الصورة. في الحالة 3 ، تقوم الطريقة المقترحة أولاً باكتشاف الحدود الخارجية لشكل الكائن ثم تغيير حجم الكائن إلى حد الصورة. تم إجراء تحقيقات تجريبية باستخدام مجموعتي بيانات صورتين قياسيتين أظهرت أن الطريقة المقترحة في الحالة 3 قد تم توضيحها لتوفير أفضل أداء لاسترجاع الصور مقارنةً بكل من 1 و2. الخلاصة تتلخص ان لالتقاط الصورة بشكل كامل خصائص تمثيل الشكل القوية للحظة زينرك ، يجب تغيير حجم كائن الشكل إلى حدود الصورة.

**الكلمات المفتاحية:** ميزات الشكل، واسترجاع صورة الشكل، لحظات زينرك